Appendix G. Mechanical VDR Form

ASC2018 Mechanical VDR Form

School/Team: University of Waterloo / Midnight Sun Solar Car Team Entry # 24

Mechanical VDR/Table of Contents

20. **Vehicle Impact Analysis:** Method: Classical (___), FEA (_x_), Testing (___)
Analysis shall be performed as per Appendix F Section F.3 and the results shall be presented in terms of factor of safety in tabulated form page_16__

Mechanical contact: Name: Devon Copeland
Email address: devon.copeland@uwmidsun.com
Phone: 226-792-7383

Project Manager: Name: Tak Alguire
Email address: tak.alguire@uwmidsun.com

1 History

Midnight Sun was founded in 1988 at the University of Waterloo. The team has produced 11 solar-powered vehicles since its inception, numbered MSI through MSXI. MSX and its predecessors have been traditional Challenger class cars. MSXI was the team's first attempt at a Cruiser class vehicle, which ultimately suffered from design issues relating to its monocoque design. With MSXII, the team has regrouped and designed a new Cruiser vehicle from the ground up, focussing strongly on reliability, safety, and manufacturability.

2 Vehicle drawings

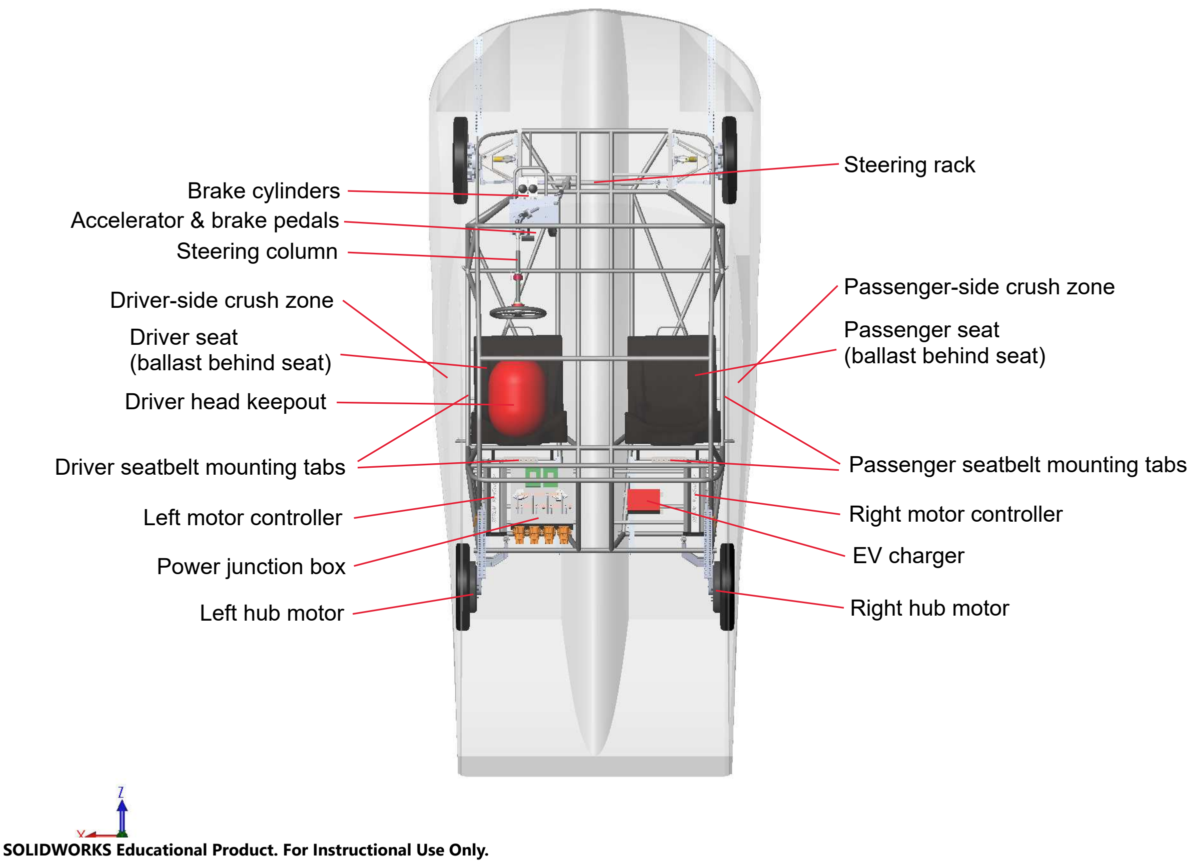

Figure 1: Top view showing major dimensions and system positions

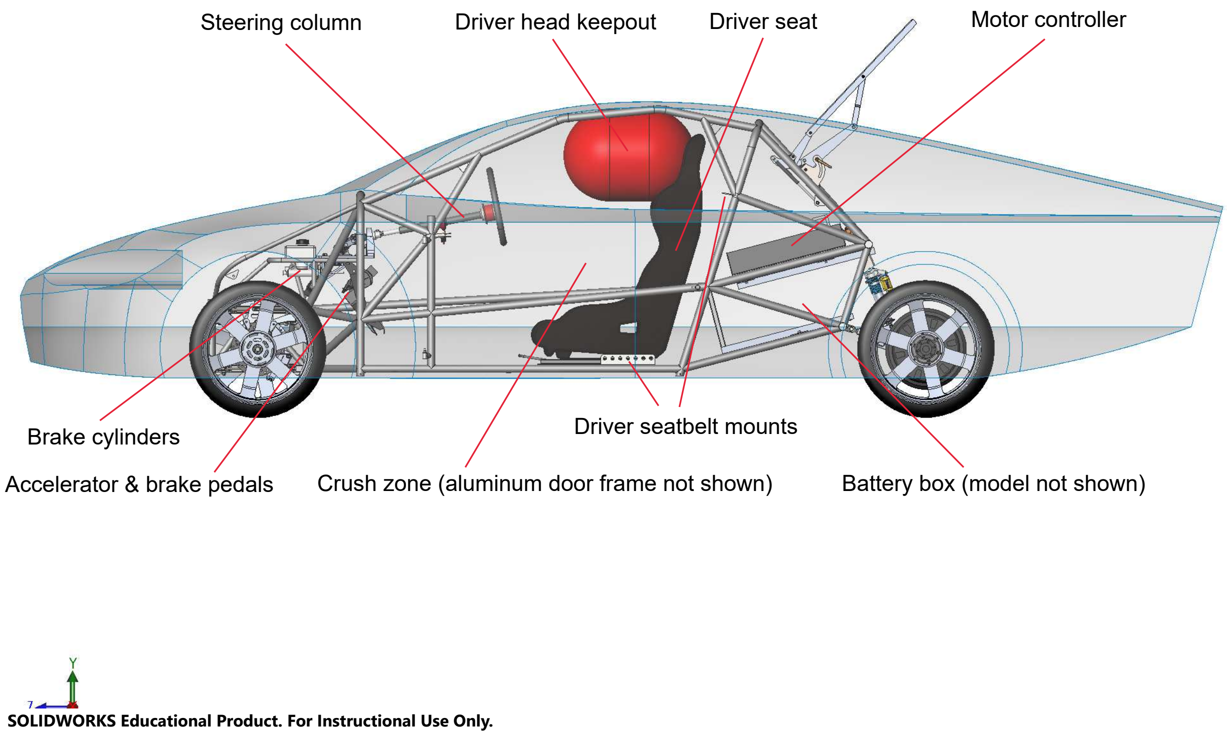

Figure 2: Side view showing major dimensions and system positions

Wheelbase	2.60 m
Track	1.60 m
Max length	4.68 m
Max width	2.02 m
Max height	1.23 m

Table 1: Table of major vehicle dimensions

3 Chassis

The chassis is a tube structure enclosing the occupant cell with small front and rear subframes to support suspension hardpoints. Smaller non-structural tube members will extend from the main frame to provide support to body panels as necessary. The majority of tubes are round, with square tubes being used only for elements intended to mount suspension and powertrain components (battery pack, motor controllers). Chassis elements use SAE 4130N chromoly tubes with diameters or side lengths ranging from 0.750" to 1.250", and wall thicknesses ranging from 0.035" to 0.065". Isometric drawings of the chassis are shown in Figures 3, 4, and 5.

Bending, cutting, and profiling of tubes was done by an external supplier. Welding of the chassis was done by a professional welder using GTAW, with support from team members for jigging and assembly. A complete welding jig was designed in CAD and manufactured using 80/20 aluminum extrusion tubing. Custom tube clamps were machined by the team to slot into jig members and fully support all chassis elements through multiple stages of assembly and welding.

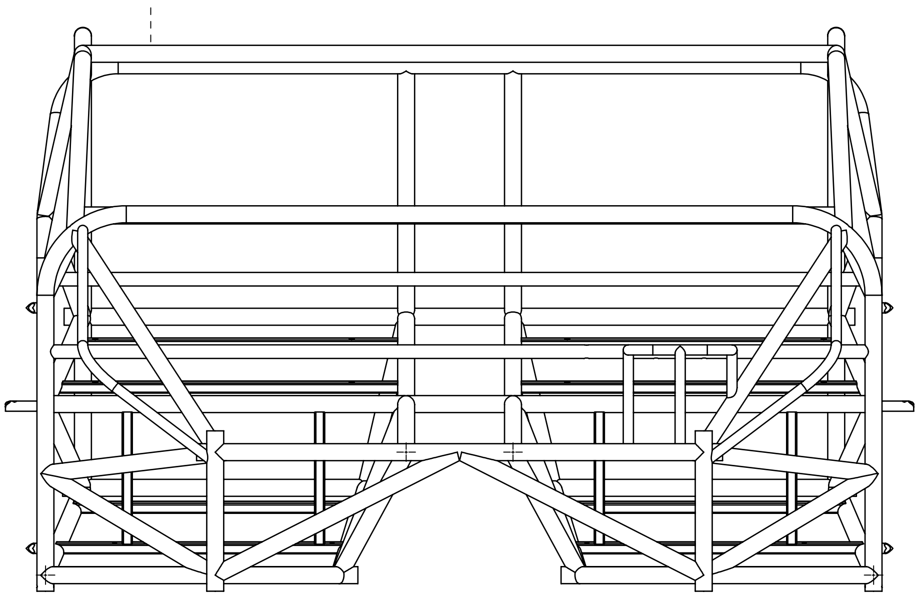

Figure 3: Chassis, front view

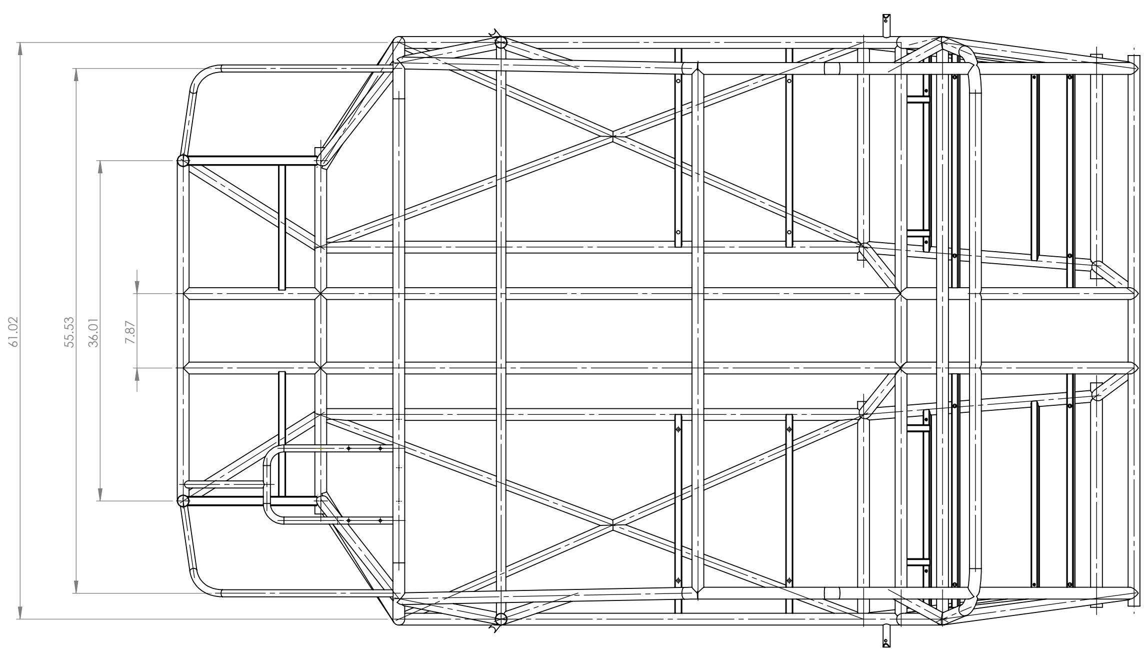

Figure 4: Chassis, top view

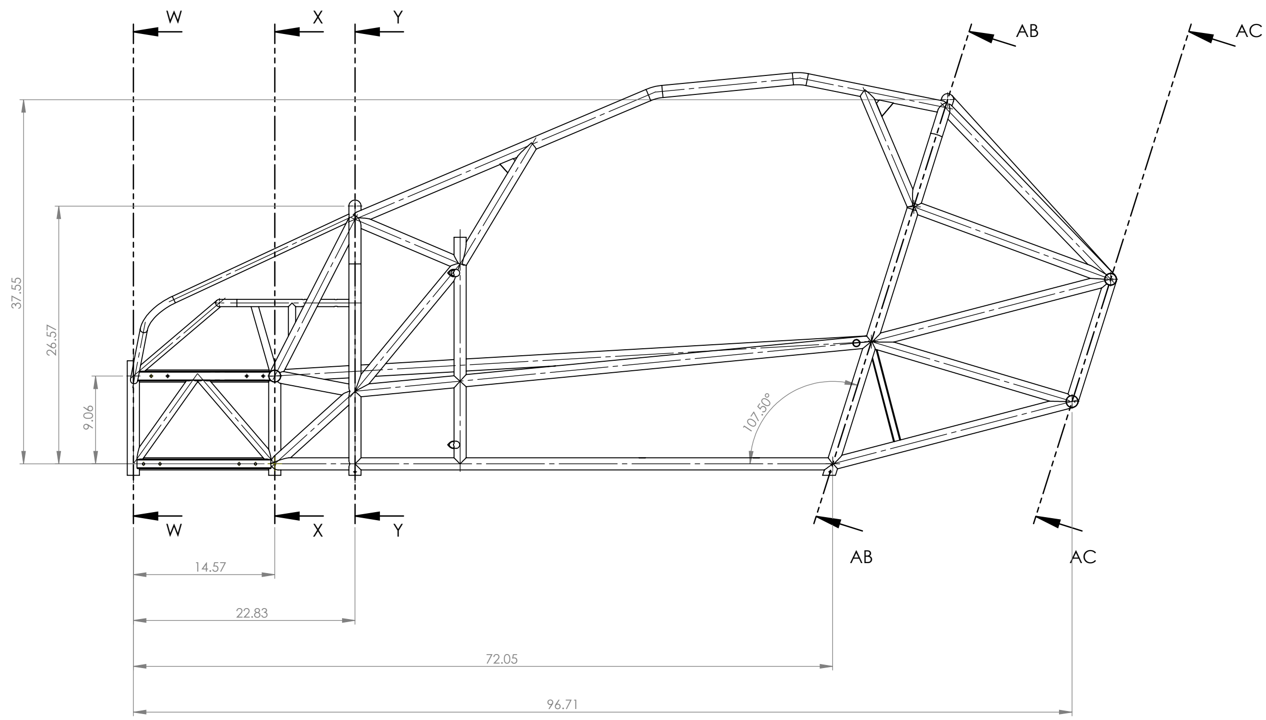

Figure 5: Chassis, side view

4 Roll cage

The roll cage is integrated into the design of the chassis members enclosing the occupant cell. For the purposes of ASC regulations, the roll cage can be considered to include the A and B pillar hoops and elements connecting these two hoops lengthwise through the car. For clarity, these elements have been highlighted in Figure 6.

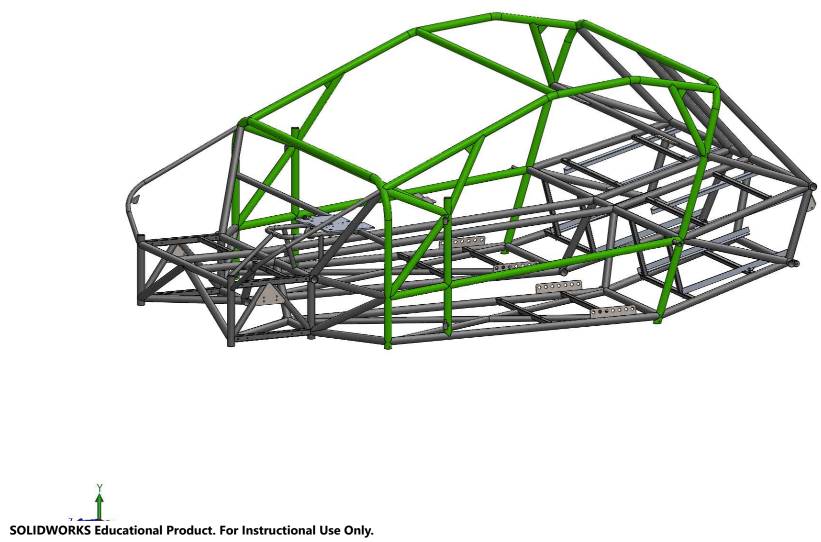

Figure 6: Chassis with roll cage elements highlighted

The vehicle's doors are designed with an aluminium planar tube structure enclosed by composite panels. Protection against side impacts is improved by the addition of 4 inches (approx. 10 cm) of energy absorbing foam (Impaxx™ 700 Series from DOW Chemical). This foam, combined with the aluminum frame and composite outer panel, together are designed to satisfy crush zone requirements for ASC. The total thickness of the door (outer face to chassis) exceeds 15 cm. The aluminum frame is designed to brace against chassis members in the event of a side impact and meets the same 5G requirement as the chassis, so that the foam layer can crush and absorb energy. FEA for the door frame is shown in Figures 36, 37, and 38 in Appendix B.

5 Seat belts

MSXII is equipped with 5-point seat belts for both occupants. Seat belt hardpoints are mounted to metal tabs welded to chassis members, shown in Figure 7. Figure 8 shows one of these tabs. Figures 9 and 10 demonstrate compliance with ASC regulations 10.3.E.

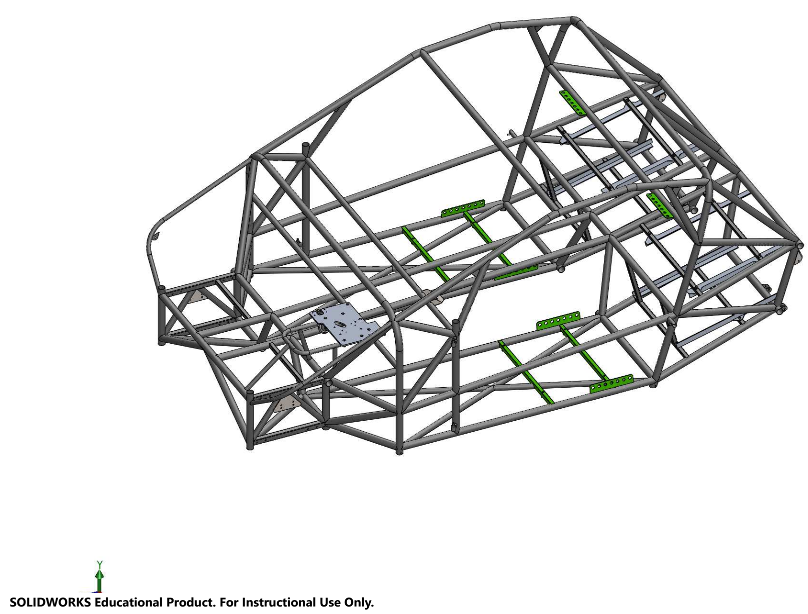

Figure 7: Chassis mounting points for seat belts

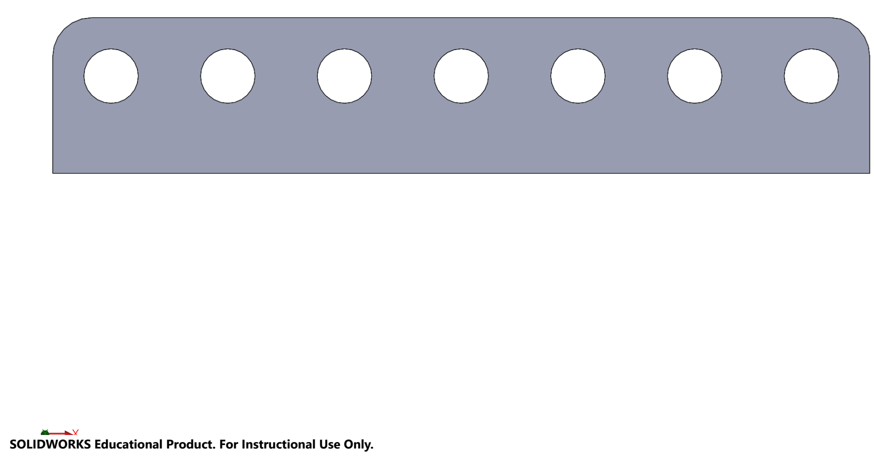

Figure 8: Single seat belt tab

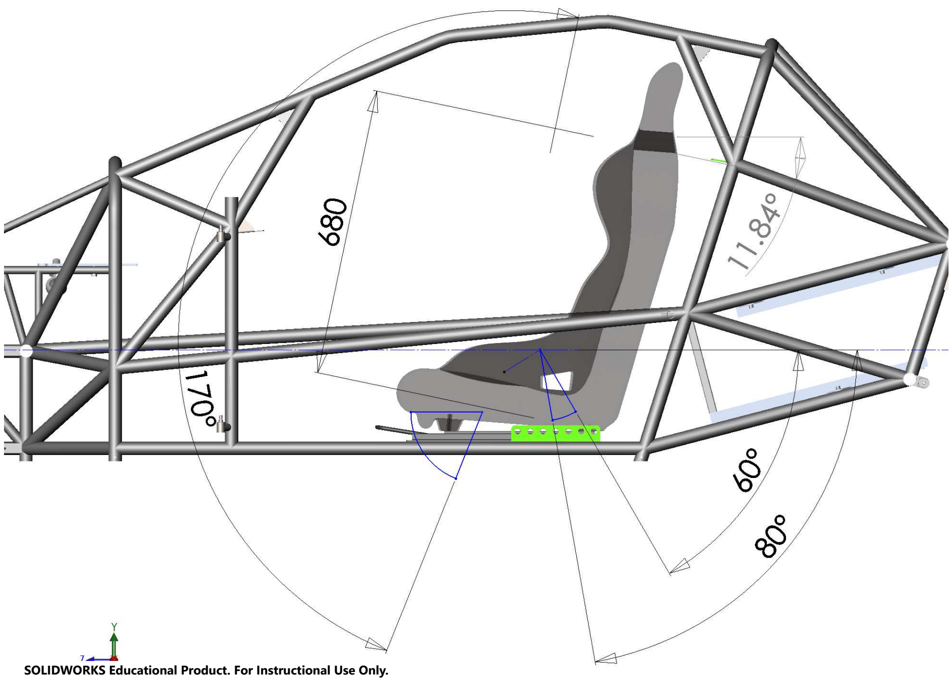

Figure 9: Side view of seat belt geometry

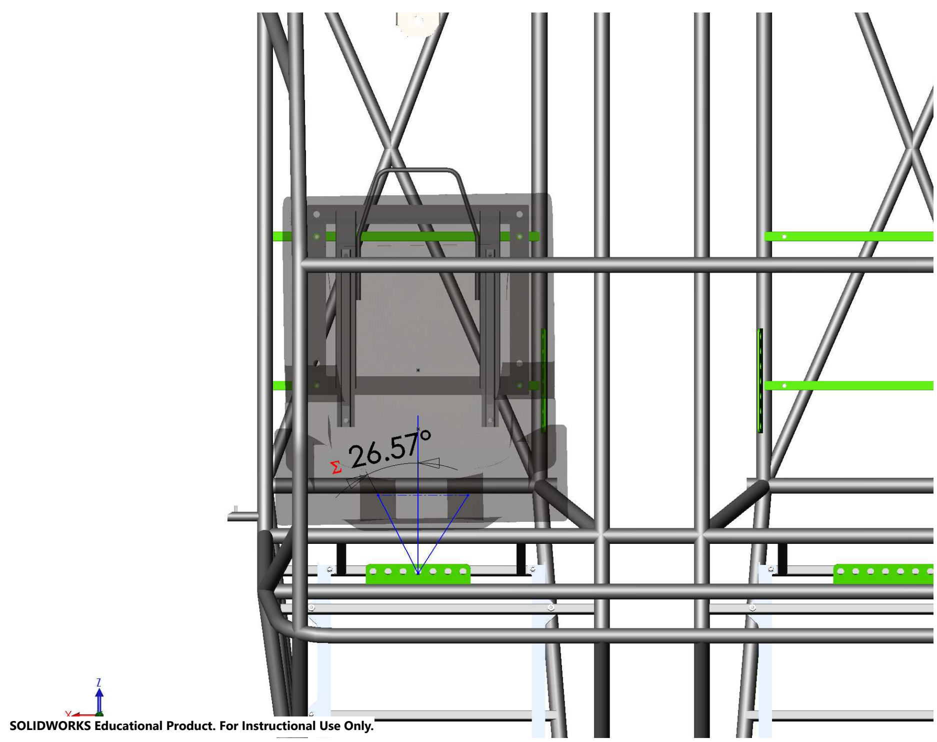

Figure 10: Top view of seat belt geometry

6 Braking system

The primary braking system is designed with dual redundant front braking, consisting of two identical systems with separate master cylinders, hydraulic lines, and calipers to each of the left and right wheels. The master cylinders are operated in unision via a single mechanical brake pedal. The brake pedal assembly is turnkey from Wilwood (part 340-15079) and has an integrated balance bar. A schematic of the primary system is shown in Figure 11.

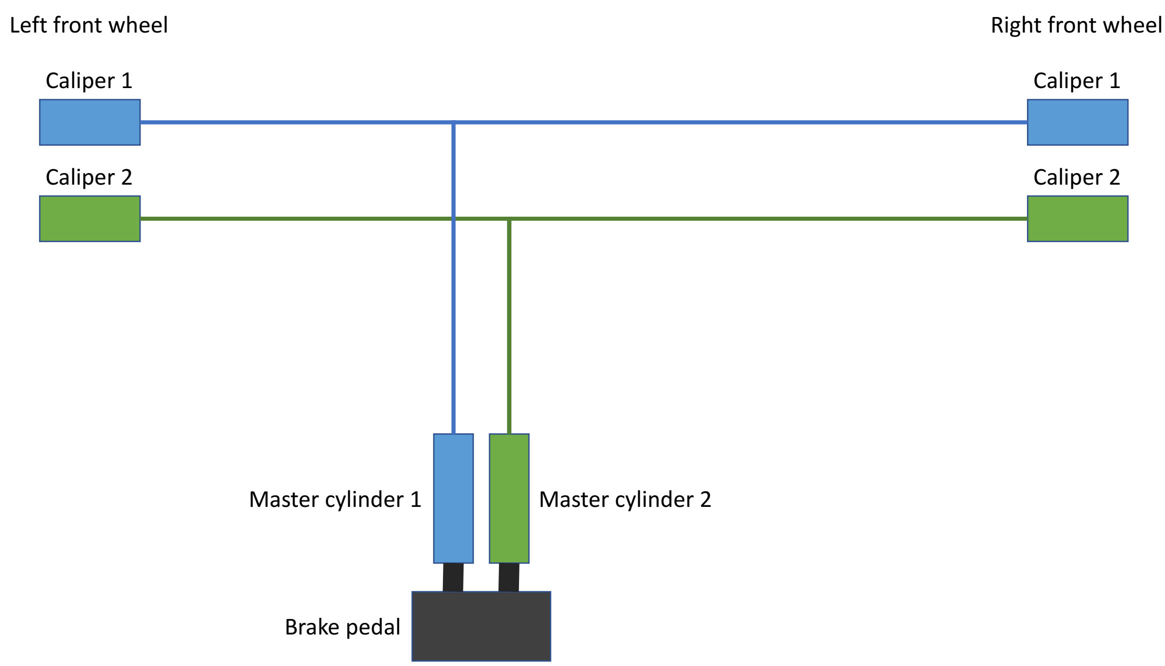

Figure 11: Schematic of primary braking system

Front brake calipers are Willwood parts 120-8374 (left) and 120-8373 (right). Willwood's website indicates the caliper pads have 2 in^2 (12.9 cm^2) contact area and 0.30" (7.6 mm) depth including the backing plate.

The master cylinders are Willwood part 206-3374. They have a 3/8"-24 outlet size which will need to be connected via a suitable brake line to the M10 x 1.25 inlets of the calipers. Brake lines will be DOT-approved hose assemblies sized for 3/8"-24 on one end and M10 on the other end via a banjo joint. The brake pedal is Willwood part 340-15079 and is mounted in the standard configuration to the left of the accelerator pedal.

Brake rotors will be custom-machined to the disk thickness and diameter supported by the Willwood calipers. All mounting geometry on the suspension upright for primary calipers are designed to position the primary calipers in the optimal positions to meet braking specifications.

The parking brake will be implemented by a cable-actuated caliper mounted at one of the front wheels. The caliper is the Tolomatic ME10LA (part number 0732-0003). It will share the same brake disk as the primary braking system but is otherwise mechanically independent. Due to unresolvable dimensioning differences between the Tolomatic and Willwood calipers, the parking brake caliper cannot be mounted perfectly as per the manufacturer's recommendations and will have only 80% overlap with the brake disk. However, this is expected to provide more than sufficient countertorque to keep the vehicle stationary as per ASC regulations 10.6. Figure 12 shows a front suspension upright with all three calipers mounted (two primary and one parking).

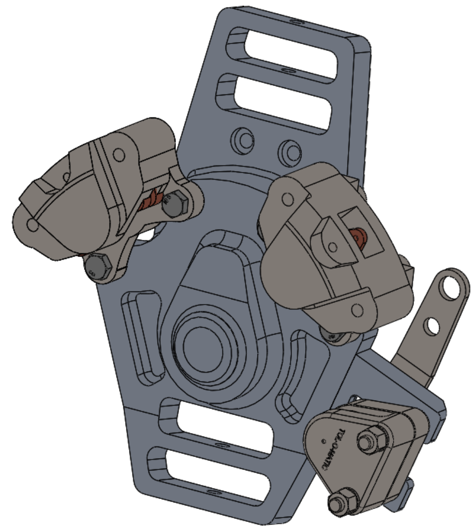

Figure 12: View of dual-primary calipers and parking caliper on front suspension upright

7 Steering system

The steering system uses a rear-steering, left-hand-drive rack and pinion from Helix (part number 188754). The system uses a collapsible steering column from Sweet Mfg. (part number 405-10310). The linkage uses dual U-joints to circumvent interfering brake system components and is shown in Figure 13. The travel of the steering rack is limited by a sleeve floating on the interface between the rack and the rack extensions. When at the maximum steering angle, the flange on the rack extension datums against the rack and pinion housing via the sleeve.

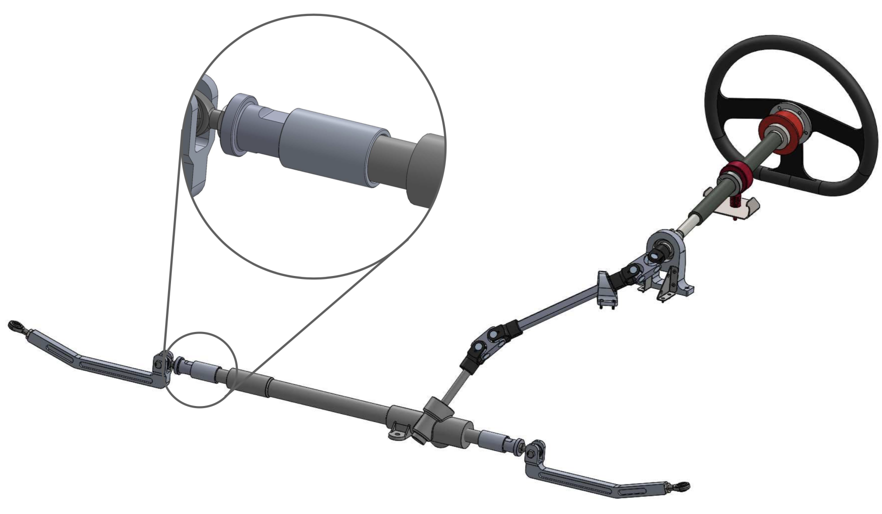

Figure 13: View of steering assembly, hardstop shown enlarged

8 Front suspension

The front suspension uses dual A-arms with an outboard dampener and coilover spring. The upper and lower control arms are custom-built from 4130 chromoly tubes. The dampener and coilover are a single integrated assembly supplied by Öhlins, sold as the TTX25, which is marketed for Formula SAE vehicles. Figures 14 and 15 show the front suspension assembly.

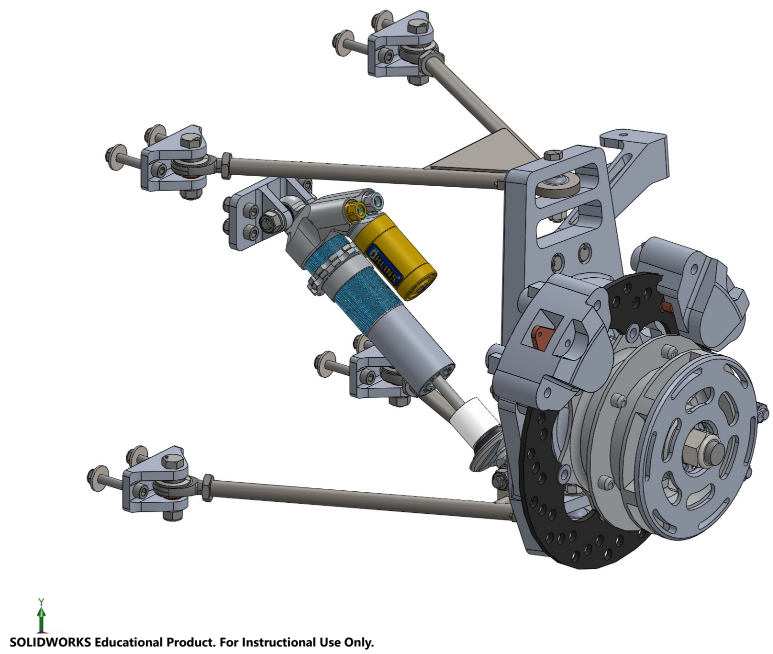

Figure 14: View of front suspension assembly (parking brake caliper obstructed by hub)

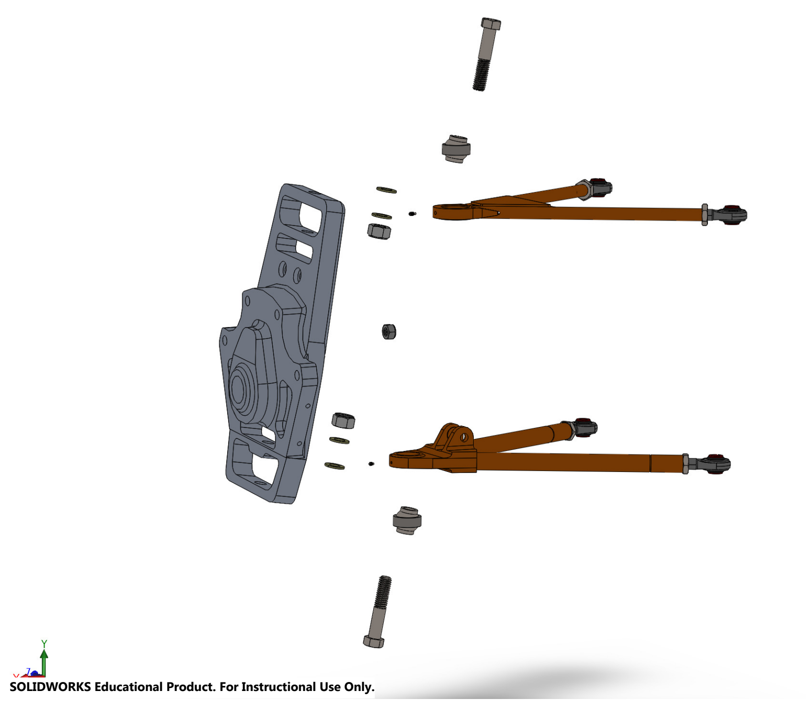

Figure 15: View of front suspension assembly, exploded

Since the front suspension lower control arm bears the majority of the shear stress from road forces, a load bearing flange has been added on the top side of the bearing seat which constrains it axially whenever in compression. This is shown in Figure 16. Both the upper and lower control arms use 7/16" spherical bearings (QA1 part number YPB7T), which are pressed into their respective chromoly bearing seats in the control arms. A CAD nominal 12 µm diametral press fit retains the spherical bearing in rare cases where the suspension rebound is sufficient to reverse the load. As an added precaution, a set screw in both the top and bottom helps to retain the bearing. Under maximum loading conditions, the stress due to bending in the bolt held in double shear was found to be 204.63 MPa. Using an SAE grade 5 bolt results in a safety factor of approximately 3.0.

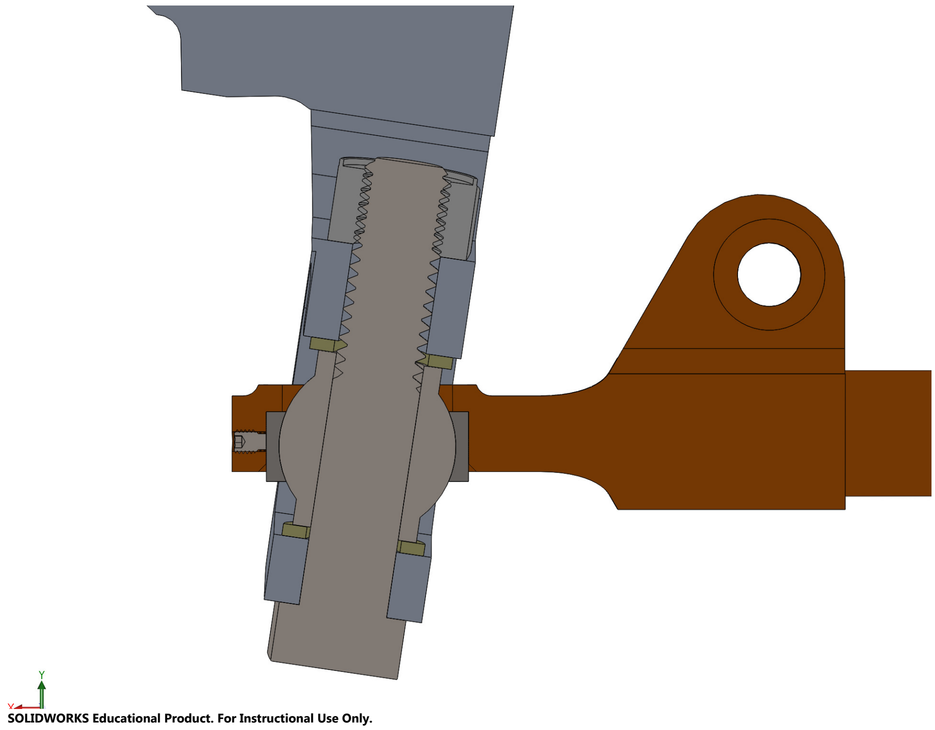

Figure 16: View of front suspension critical rod end, cross-section

9 Rear suspension

The rear suspension uses independent trailing arms mounted outwards from the rear of the chasssis. The trailing arm itself is custom-machined and mounts the same Öhlins TTX25 shock absorber as the front suspension. Figure 17 shows the rear suspension assembly.

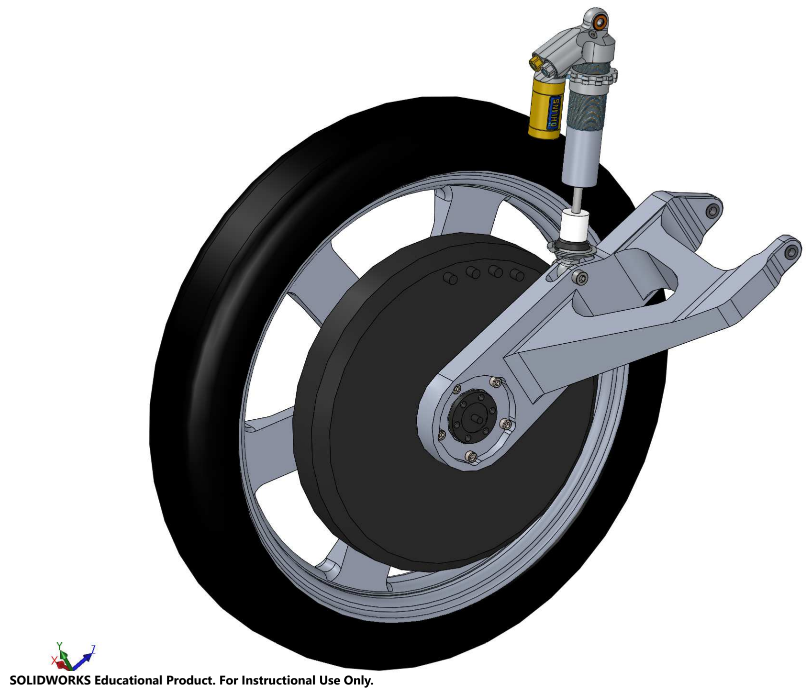

Figure 17: View of rear suspension assembly

The rear suspension pivots about plain bearings pressed into the trailing arm. Stress in the trailing arm at the plain bearings was simulated using FEA as shown Figure 17 to verify sufficient safety factor. The lack of rod ends allows a smaller interface with the rear suspension clevis mounts, which would otherwise need to be sized significantly larger.

10 Tires and rims

MSXII is designed to use Schwalbe Energizer Solar 51L tires. These tires have a max load rating of 195 kg and are designed specifically for light electric vehicles travelling at highway speeds (120 km/h). Their maximum inflation pressure is 70 PSI.

Custom rims meeting the geometric specifications of the Energizer Solar tires were designed by the team and CNC milled out of 6061 aluminium.

11 Crush Zone

MSXII has been designed with an extruded polystyrene foam (EPS) crush zone, designed to absorb the energy of a 5G impact to the doors on both sides of the vehicle. The EPS crush foam is enclosed between the outer door panel and the inner door frame, made of 6061-T6 aluminum tubing, and the inner door panel. EPS foam does not shatter under loading, ensuring no fragments enter the driver cell in the event of a collision.

12 Battery Box

Two battery packs are implemented in the design of MSXII: a ”slave” pack providing exclusively power and some auxiliary electrical control, and a ”master” pack, containing both battery cells and electrical boards which control the battery system. The full details of the electrical side of the pack construction is detailed in the appropriate electrical system VDR. From a mechanical standpoint, both packs have identical designs and mounting features.

The pack is constructed from 1/4" thick honeycomb fibreglass composite panels, bonded to a welded aluminum frame with an inert epoxy. Fibreglass is electrically insulating, and hence isolates the internals of both battery boxes from the external metal frames and surrounding chassis. The aluminum frame has welded mounting tabs on both the top and bottom of the box, which interface with matching mounting tabs welded to the chassis above and below the box. FEA with a 20G impact load on all mounting tabs yielded safety factors around 1.5-2. This high loading was applied to assure compliance with World Solar Challenge regulations - well above the required 5G impact loading. The mounting tabs provide a location on both sides of each box (master and slave) for a fastener and locking nut to secure the box to the chassis and prevent the battery enclosure from becoming loose during an impact or rollover event.

13 Array Panel Attachment

Both the front and rear array panels are attached to the chassis of MSXII on a custom 6-bar linkage, made from aluminum members and actuated with a gas spring. The upper member of the hinges are attached to the respective array panel with epoxy resin. This serves as the primary method of array attachment to the chassis of the vehicle. As a secondary method to provide redundancy to the first method of array attachment, aluminum aircraft cable is connected to each panel individually with epoxy resin, and connected to the chassis. This satisfies the regulation, as each attachment method is independent of one another.

14 Fasteners

All structural fasteners used in the vehicle are at least of metric grade 8.8, with most being grade 10.9 or 12.9. Fujilok (self-locking) nuts from Spaenaur are used in all structural applications. The bolts mounting each motor are safety threaded as required for all blind-holes. A complete Bill of Materials listing every fastener used in the car is available upon request.

15 Vehicle impact analysis

Finite element analysis was performed using ANSYS on the chassis, doors, and all suspension and steering components (downstream from the rack and pinion). FEA of the chassis and door followed the specifications provided by the ASC regulations. A general methodology was to fix a solid beam or wall in space and apply a 5G acceleration to the chassis against it. Images for FEA simulations of each requested scenario are shown in Appendix B.

Worst-case loading forces on each wheel were used to derive appropriate contraints and forces for FEA simulation of the suspension and steering system. A complete derivation and summary of loading forces on each wheel is given in Appendix A. Images of all FEA simulations for suspension and steering are available in Appendix C.

15.1 Front suspension

15.1.1 Clevises

Hand calculations were used to resolve the forces from the road as loading onto the clevises. The back face of the clevis was constrained with compresion only support. Cylindrical supports were used for the bolt holes and fastener pretension was added. Frictional contacts were added between the fasterners and the clevis.

15.1.2 Upper control arms

Contacts were modeled between the control arm tubes and the bearing plate. Forces were applied to the bearing plate based on hand calculations.

15.1.3 Lower control arms

Contacts were modeled between the control arm tubes and the mounting tabs on the coilover clevis. Forces were applied to the profile that the bearing sits in, based off of hand calculations.

15.1.4 Uprights

A dummy wheel was modeled to which forces were applied. The dummy wheel contacted the spindle with a frictional contact which then applied a load to the upright. The brake forces were appled to the caliper mounting holes, assuming only one caliper was providing all braking force.

15.1.5 Spindles

A dummy wheel was modeled to which forces were applied. The dummy wheel contacted the spindle with a frictional contact which then applied a load to the upright.

15.1.6 Upper bearing plates

Contacts were modeled between the control arm tubes and the bearing plate. Forces were applied to the bearing plate based on hand calculations.

15.1.7 Coilover control arm tabs

The maximum force on the front wheel was resolved as a compressive load in the coilover and applied to this tab.

15.1.8 Coilover mounting plates

Hand calculations were used to resolve the forces from the road as loading onto the clevises. For this simulation a frictional contact was added between the clevis and the mounting plate. Dummy chassis tubes were modeled behind the mounting plate and welded edges were fixed.

15.2 Rear suspension

15.2.1 Clevises

The worst case of four loading scenarios was taken (2 clevis positions, each with either the inside or outside wheel when rounding a corner). It was assumed that all lateral force was applied to a single clevis because otherwise this is a statically indeterminate problem on paper.

15.2.2 Coilover tabs

The maximum normal force and acceleration force on the rear wheel was resolved as a compressive load in the coilover and applied to this tab.

15.2.3 Trailing arms

Similar to the front suspension, the trailiing arm was simulated using a dummy wheel model. A force was applied to the contact patch and supports were added to the plain bearings and coilover clevis on the trailing arm.

15.3 Steering

15.3.1 Steering arms

A compression support was added on the face datuming off of the upright. The maximum lateral force on the tire during 1G cornering was resolved as a torque on the upright. This torque was applied by a bearing load acting at the end of the steering arm.

15.3.2 Tie rods

A similar analysis to that for the steering arm was used. Force was applied to one end of the tie rod while the other remained fixed. Both sides of the tie rod were tested with an applied force and fixed support.

15.4 Results

All FEA results for suspension and steering components are summarized in Table 2.

Part Number	Part Name	Material	Max Stress (MPa)	Safety Factor
MS00015	Coilover Clevis	Aluminum, 7075	147	3.4
MS00029	Upper Control Arm Clevis	Aluminum, 7075	191	2.6
MS00102	Lower Control Arm Clevis	Aluminum, 7075	198	2.5
MS00017	Upper Control Arm	Chromoly Steel, 4130	199	2.3
MS00018	Lower Control Arm	Chromoly Steel, 4130	226	2.0
MS00019	Upright	Aluminum, 7075	210	2.4
MS00020	Spindle	Chromoly Steel, 4140	177	2.3
MS00030	Upper Bearing Plate	Chromoly Steel, 4130	141	3.3
MS00036	Coilover Control Arm Tab	Chromoly Steel, 4130	159	2.9
MS00038	Coilover Mounting Plate	Chromoly Steel, 4130	147	3.1
MS00086	Rear Suspension Clevis Mount	Chromoly Steel, 4130	231	2.0
MS00047	Rear Suspension Coilover Tab	Chromoly Steel, 4130	147	3.1
MS00065	Trailing Arm	Aluminum, 7075	263	1.9
MS00074	Steering Arm	Aluminum, 6061-T6	77	3.5
MS00101	Tie Rod	Aluminum, 6061-T6	41	6.6

Table 2: Summary of FEA results for suspension and steering components

A Loading conditions

FEA of the chassis, suspension, and steering system was done using ANSYS software. Loading conditions were derived from both ASC requirements and real-world scenarios. Assuming a smooth driving surface, the largest normal force acting on the front tire will occur while braking in a turn. Similarly, the largest normal force acting on the rear tire will occur while accelerating in a turn. To approximate these loading condition, the a superposition of two static half car models is used; one for cornering and one for hard braking.

Table 3 lists vehicle parameters that are relevant in determining the loading conditions in the suspension. The mass and moment of inertia were computed using CAD software.

Mass (M)	550	kg
Wheelbase	2.60	m
Track	1.60	m
Tire Diameter	0.53	m
Wheel Assembly Moment of Inertia (J_w)	0.25	kg m^2
Distance from Front Wheel to CoG (a)	1.32	m
Distance from Front Wheel to CoG (b)	1.28	m
Distance from Road to CoG (h)	0.52	m
Full Wheel Travel in Compression	45	mm
Front Coilover Angle from Vertical	40	°
Rear Coilover Angle from Vertical	30	°

Table 3: Important vehicle parameters

A.1 Braking

Figure 18 shows a free body diagram of a half car model undergoing braking. The required braking force can be approximated as follows:

$$F_{\text{braking}} = F_{\text{Nf}} + F_{\text{Nr}} = Mg = (550\,\text{kg})(9.81\,\text{m}\,\text{s}^{-2}) = 5.40\,\text{kN} \tag{1}$$

From Figure 18, summing the moments about the centre of gravity and the vertical forces results in the following equations:

$$aF_{\text{Nf}} = hF_{\text{braking}} + bF_{\text{Nr}} \tag{2}$$

$$F_{\text{Nf}} + F_{\text{Nr}} = Mg \tag{3}$$

Solving for the front normal force:

$$\begin{aligned} aF_{\text{Nf}} &= hF_{\text{braking}} + b(Mg - F_{\text{Nf}}) \\ F_{\text{Nf}} &= \frac{hF_{\text{braking}} + bMg}{a+b} = \frac{(0.52\,\text{m})(5.40\,\text{kN}) + (1.28\,\text{m})(550\,\text{kg})(9.81\,\text{m}\,\text{s}^{-2})}{(1.32\,\text{m}) + (1.28\,\text{m})} = 3.74\,\text{kN} \end{aligned} \tag{4}$$

Note that 3.74 kN is for both front wheels. Therefore there is approximately 1.87 kN of normal force on each front tire during hard braking.

A.2 Acceleration

MSXII uses NGM SCM-150 motors which have a peak torque of 135 N m. From this torque value and a number of other vehicle parameters the vehicle's maximum acceleration can be calculated as follows:

$$a = \frac{F_w}{\frac{1}{2}M} \tag{5}$$

$$\alpha_w = \frac{T_m - F_w r}{J_w} \tag{6}$$

$$\alpha_w = ar \tag{7}$$

where a is the acceleration of the vehicle, F_w is the friction force acting on a single tire while accelerating, J_w is the moment of inertia of the wheel assembly, r is the radius of the tire, T_m is the torque from the motor and α_w is the angular acceleration of the wheel.

Rearranging the above three equations, the acceleration of the vehicle can be expressed as a function of motor torque as follows:

$$a = \frac{T_m r}{\frac{1}{2}Mr^2 + J_w}$$
$$a = \frac{(135\,\mathrm{N\,m})(0.27\,\mathrm{m})}{\frac{1}{2}(550\,\mathrm{kg})(0.27\,\mathrm{m}^2)^2 + 0.25\,\mathrm{kg\,m}^2} = 1.80\,\mathrm{m\,s}^{-2} \tag{8}$$

Solving for friction force on a single rear tire:

$$F_w = Ma = (550\,\mathrm{kg})(1.80\,\mathrm{m\,s}^{-2}) = 990\,\mathrm{N} \tag{9}$$

The resulting normal force on the rear wheels can be calculated as follows:

$$bF_{\mathrm{Nr}} = hF_{\mathrm{w}} + a(Mg - F_{\mathrm{Nr}})$$
$$F_{\mathrm{Nr}} = \frac{hF_{\mathrm{w}} + aMg}{a+b} = \frac{(0.52\,\mathrm{m})(990\,\mathrm{N}) + (1.32\,\mathrm{m})(550\,\mathrm{kg})\left(9.81\,\mathrm{m\,s}^{-2}\right)}{(1.32\,\mathrm{m}) + (1.28\,\mathrm{m})} = 2.94\,\mathrm{kN} \tag{10}$$

Note that 2.94 kN is for both rear wheels. Therefore there is approximately 1.47 kN of normal force on each rear tire during maximum acceleration.

A.3 Cornering

ASC regulations require simulations of a 1G turn, at minimum. This corresponds to the following lateral force:

$$F_{\mathrm{steer}} = Mg = (550\,\mathrm{kg})(9.81\,\mathrm{m\,s}^{-2}) = 5.40\,\mathrm{kN} \tag{11}$$

Additionally, the diameter of several highway exit ramps around the University of Waterloo were measured on satellite maps. The recommended speed limit on these exits is 50 km h^{-1}. Assuming a worst case scenario where the vehicle takes an exit with a 100 m diameter at 80 km h^{-1} (22.22 m s^{-1}), the required lateral force required to navigate this corner can be found as follows:

$$F_{\mathrm{steer}} = \frac{Mv^2}{r} = \frac{(550\,\mathrm{kg})(22.22\,\mathrm{m\,s}^{-1})^2}{50\,\mathrm{m}} = 5.43\,\mathrm{kN} \tag{12}$$

This corresponds nearly identically to a 1G turn. Since the lateral force required in the second scenario is slightly higher, 5.34 kN will be used as the worst case cornering force.

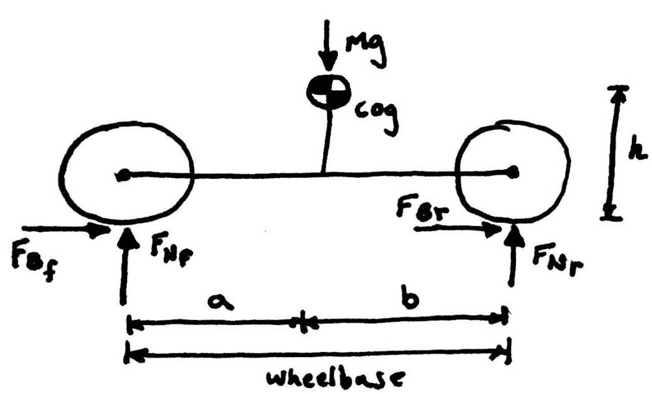

Figure 18: Free body diagram of vehicle braking

Using the half car model shown if Figure 19, summing the moments about the centre of gravity and the vertical forces results in the following equations:

$$\frac{1}{2}L_{\text{track}}F_{\text{No}} = hF_{\text{steer}} + \frac{1}{2}L_{\text{track}}F_{\text{Ni}} \tag{13}$$

$$F_{\text{No}} + F_{\text{Ni}} = Mg \tag{14}$$

Solving for the outside wheel normal force:

$$\begin{aligned}\frac{1}{2}L_{\text{track}}F_{\text{No}} &= hF_{\text{steer}} + \frac{1}{2}L_{\text{track}}(Mg - F_{\text{Ni}}) \\ F_{\text{No}} &= \frac{hF_{\text{steer}} + \frac{1}{2}L_{\text{track}}Mg}{L_{\text{track}}} = \frac{(0.52\,\text{m})(5.43\,\text{kN}) + (0.80\,\text{m})(550\,\text{kg})\left(9.81\,\text{m}\,\text{s}^{-2}\right)}{1.60\,\text{m}} = 4.46\,\text{kN}\end{aligned} \tag{15}$$

Solving for the inside wheel normal force:

$$F_{\text{Ni}} = Mg - F_{\text{No}} = (550\,\text{kg})\left(9.81\,\text{m}\,\text{s}^{-2}\right) - 4.46\,\text{kN} = 0.93\,\text{kN} \tag{16}$$

Note that the forces above are for both front and rear outside wheels. Assuming the force is evenly split between the front and rear, there is approximately 2.23 kN of normal force on each outside tire and 0.47 kN for each inside tire during maximum cornering.

A.4 Bump

As stipulated in the ASC 2018 regulations, the analysis for suspension and steering must include loading considerations for a 2G bump. We interpret this requirement as the body of the vehicle accelerating upwards at 2G, in which case the additional normal force subjected to a single tire can be expressed as follows:

$$F_{\text{N,bump}} = \frac{2Mg}{4} = \frac{2(9.81\,\text{m}\,\text{s}^{-2})(550\,\text{kg})}{4} = 2.70\,\text{kN} \tag{17}$$

A.5 Superposition

The braking, accelerating, and cornering conditions subject the wheels to normal forces that differ from those experienced when the car is at rest. The change in normal force for each loading condition can be expressed

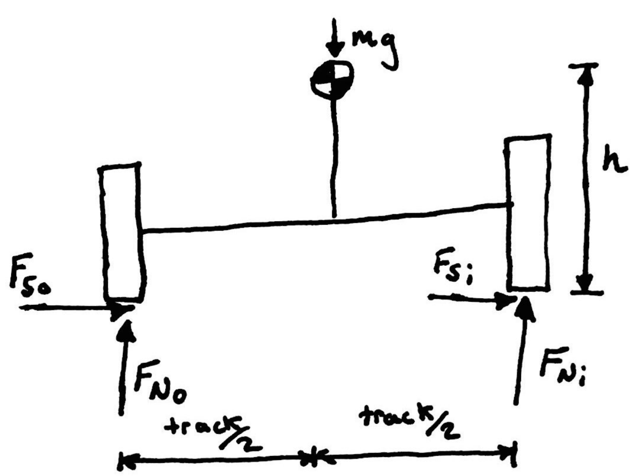

Figure 19: Free body diagram of vehicle cornering

as follows:

$$\Delta F_{\text{Nf,braking}} = F_{\text{Nf,braking}} - \frac{Mg}{4} = 1.87\,\text{kN} - 1.35\,\text{kN} = 0.52\,\text{kN} \tag{18}$$

$$\Delta F_{\text{Nr,accelerating}} = F_{\text{Nf,braking}} - \frac{Mg}{4} = 1.47\,\text{kN} - 1.35\,\text{kN} = 0.12\,\text{kN} \tag{19}$$

$$\Delta F_{\text{No,cornering}} = F_{\text{No,cornering}} - \frac{Mg}{4} = 2.23\,\text{kN} - 1.35\,\text{kN} = 0.88\,\text{kN} \tag{20}$$

$$\Delta F_{\text{Ni,cornering}} = F_{\text{No,cornering}} - \frac{Mg}{4} = 0.47\,\text{kN} - 1.35\,\text{kN} = -0.88\,\text{kN} \tag{21}$$

$$\Delta F_{\text{N,bump}} = F_{\text{N,bump}} - \frac{Mg}{4} = 2.70\,\text{kN} - 1.35\,\text{kN} = 1.35\,\text{kN} \tag{22}$$

To approximate the worst case loading condition, a superposition of the changes in normal force and the nominal normal force is applied. Note that the nominal force used is the same for each wheel, which assumes a centre of gravity approximately centred along the wheelbase.

$$F_{\text{Nfi,max}} = \Delta F_{\text{Nf,braking}} + \Delta F_{\text{Ni,cornering}} + 2F_{\text{N,nominal}} = 0.52\,\text{kN} - 0.88\,\text{kN} + 2.70\,\text{kN} = 2.34\,\text{kN} \tag{23}$$

$$F_{\text{Nfo,max}} = \Delta F_{\text{Nf,braking}} + \Delta F_{\text{No,cornering}} + 2F_{\text{N,nominal}} = 0.52\,\text{kN} + 0.88\,\text{kN} + 2.70\,\text{kN} = 4.10\,\text{kN} \tag{24}$$

$$F_{\text{Nri,max}} = \Delta F_{\text{Nr,braking}} + \Delta F_{\text{Ni,cornering}} + 2F_{\text{N,nominal}} = 0.12\,\text{kN} - 0.88\,\text{kN} + 2.70\,\text{kN} = 1.94\,\text{kN} \tag{25}$$

$$F_{\text{Nro,max}} = \Delta F_{\text{Nr,braking}} + \Delta F_{\text{No,cornering}} + 2F_{\text{N,nominal}} = 0.12\,\text{kN} + 0.88\,\text{kN} + 2.70\,\text{kN} = 3.70\,\text{kN} \tag{26}$$

A.6 Summary

Table 4 summarizes the loading conditions used for static structural FEA simulations on the suspension and steering components. Note that the direction of the force corresponds's with the global coordinate system of the MSXII and the vectors shown in Figure 20. The assemblies shown are for the driver's side of the vehicle

Table 4: Summary of worst case loading conditions

Worst Case Loading	F_x (kN)	F_y (kN)	F_z (kN)
Braking & Cornering (Inside Front Wheel)	2.72	2.34	2.70
Braking & Cornering (Outside Front Wheel)	-2.72	4.10	2.70
Accelerating & Cornering (Inside Rear Wheel)	2.72	1.94	0.99
Accelerating & Cornering (Outside Rear Wheel)	-2.72	3.70	0.99

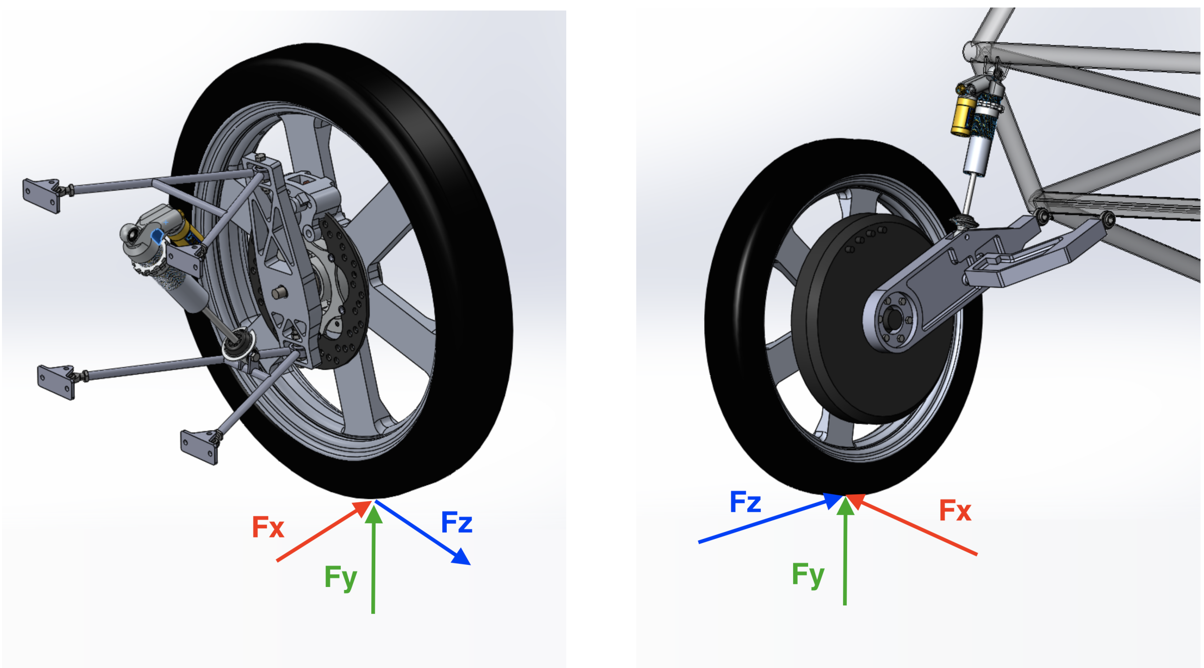

(a) Font suspension (b) Rear suspenion

Figure 20: Suspension coordinate system

B FEA images for chassis and door

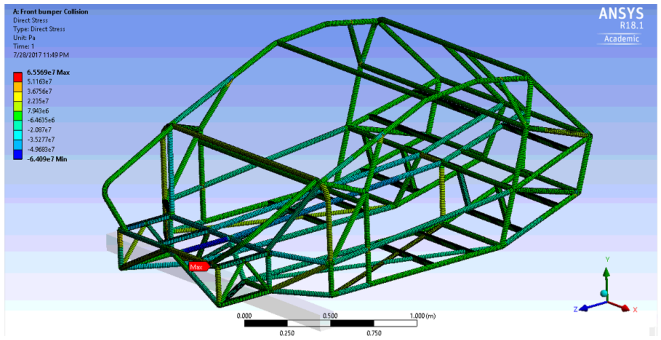

Figure 21: Front bumper collision

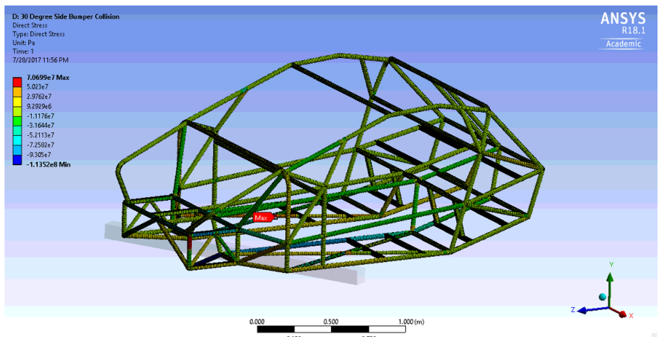

Figure 22: Front bumper 30 degree collision

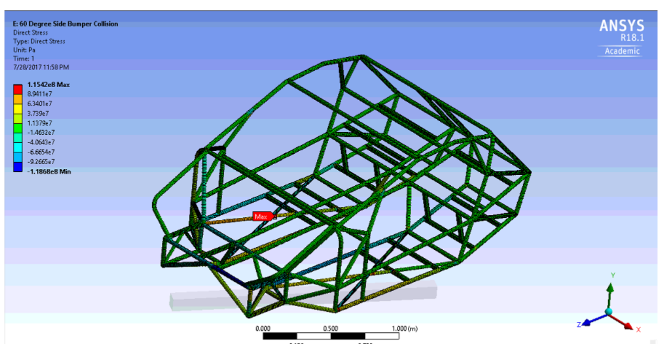

Figure 23: Front bumper 60 degree collision

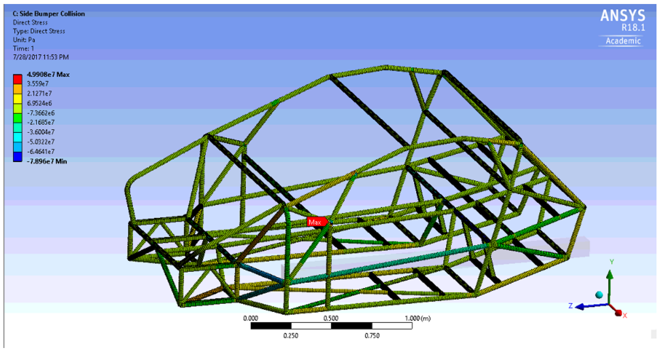

Figure 24: Side bumper collision

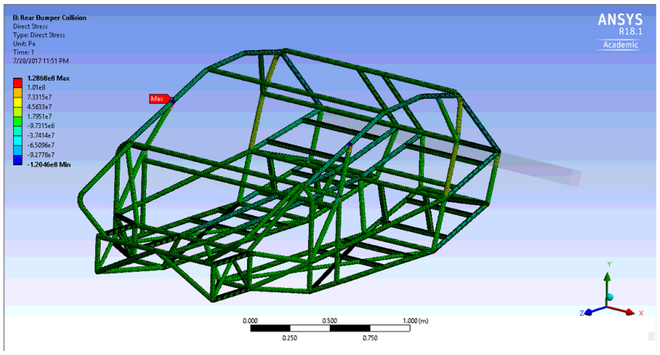

Figure 25: Rear bumper collision

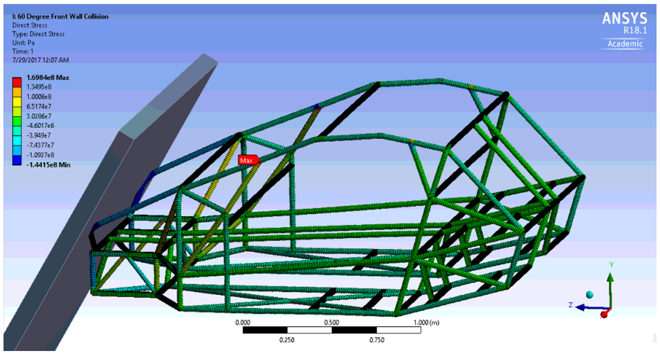

Figure 26: Hood 60 degree collision

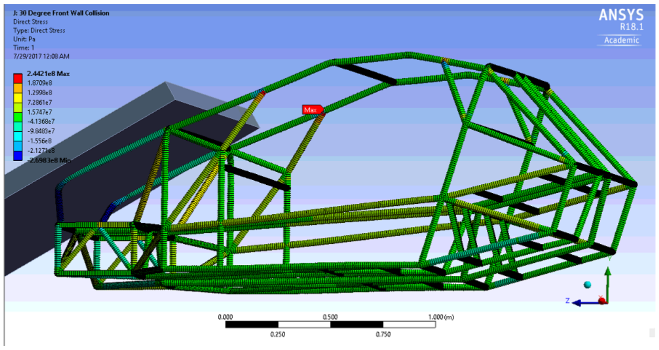

Figure 27: Hood 30 degree collision

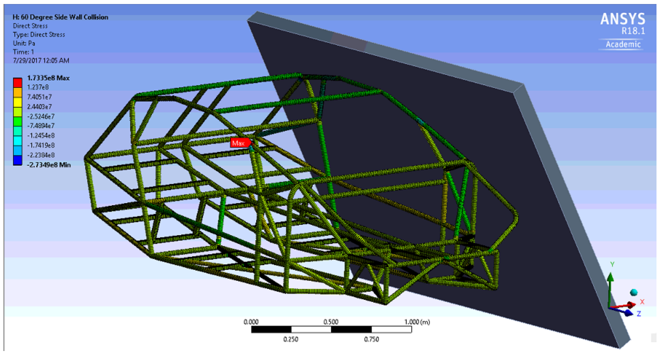

Figure 28: Side 60 degree collision

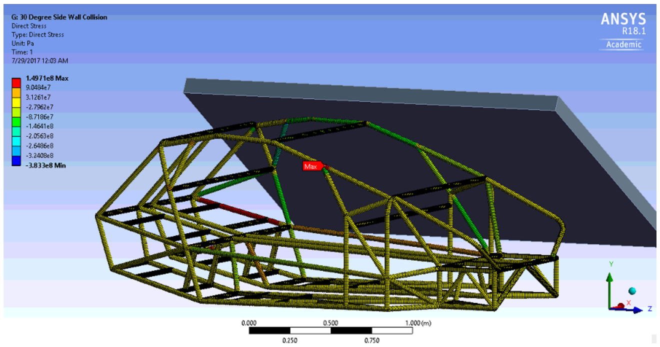

Figure 29: Side 30 degree collision

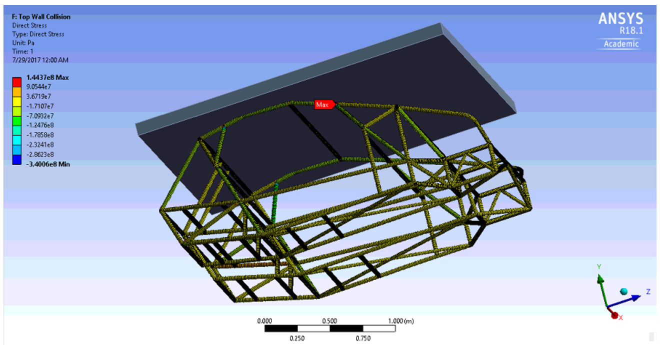

Figure 30: Roof top collision

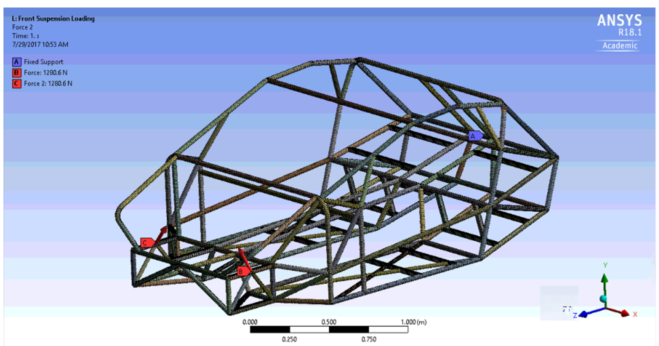

Figure 31: Vehicle rest front subframe loading

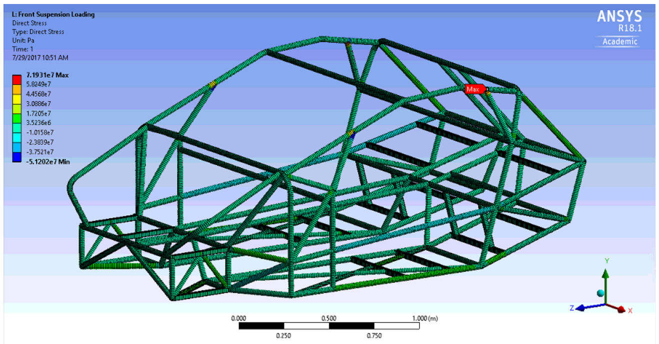

Figure 32: Vehicle rest front subframe stress

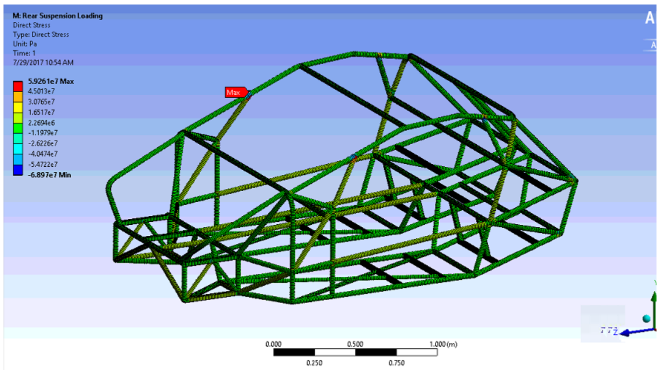

Figure 33: Vehicle rest rear subframe stress

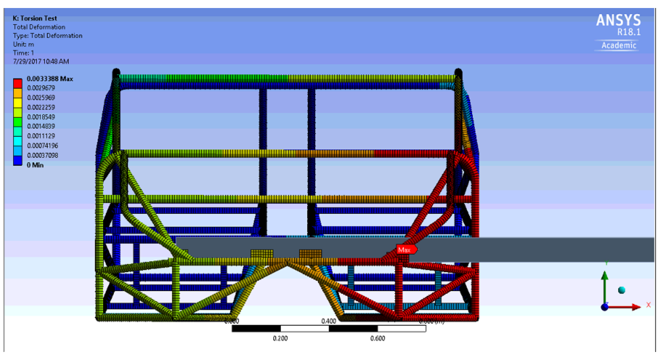

Figure 34: Torsion test, deformation

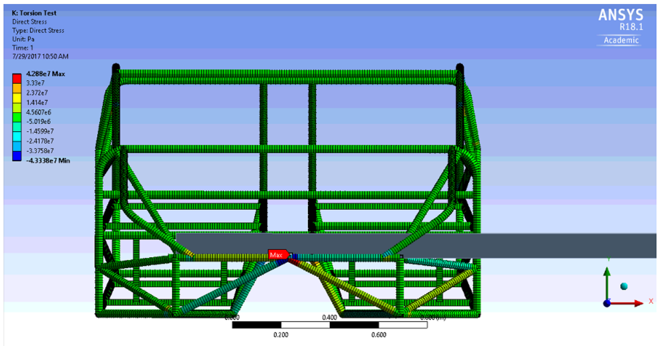

Figure 35: Torsion test, stress

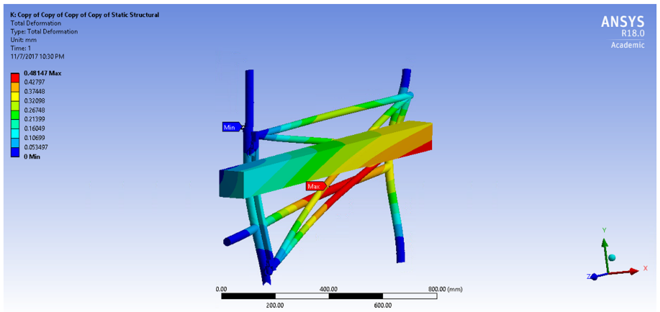

Figure 36: Door side impact displacement

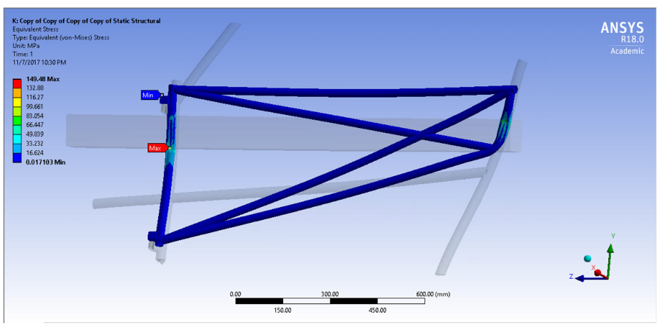

Figure 37: Door side impact stress

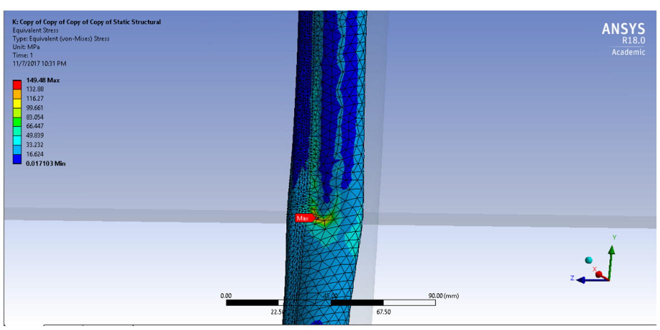

Figure 38: Door side impact stress, zoomed

C FEA images for suspension and steering

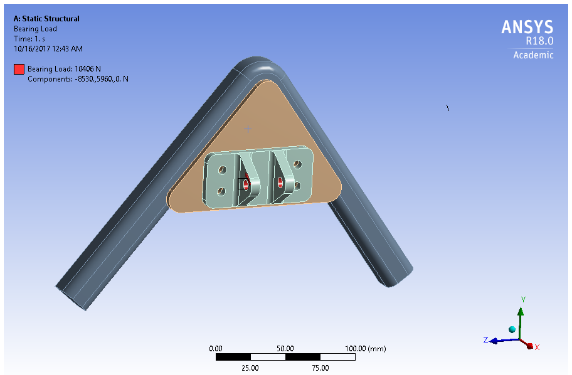

(a) Setup

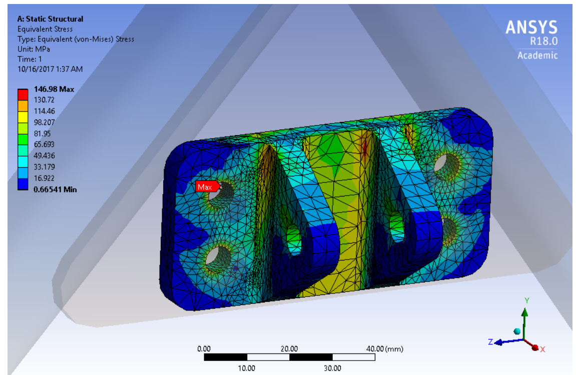

(b) Stress

Figure 39: Coilover clevis

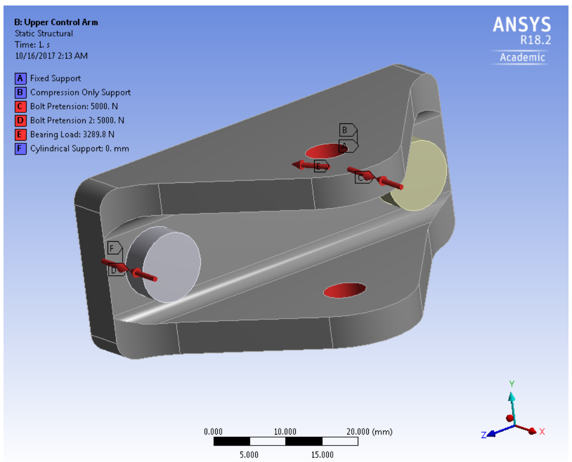

(a) Setup

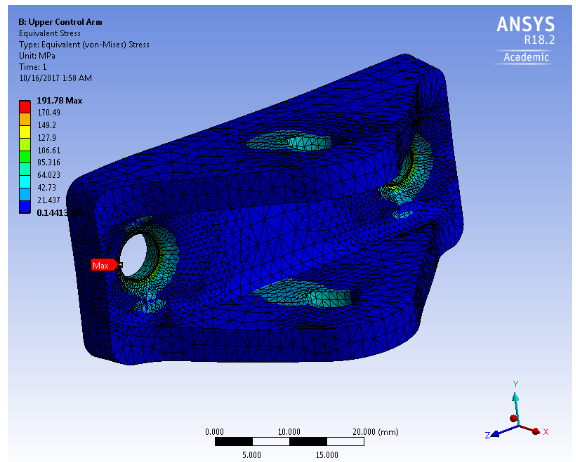

(b) Stress

Figure 40: Upper control arm clevis

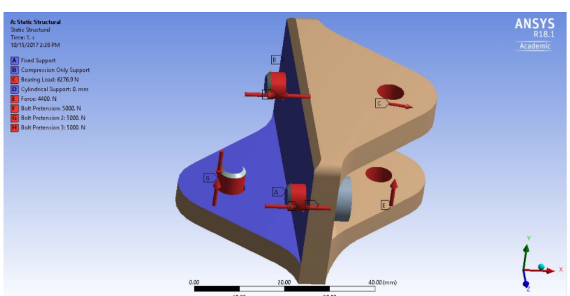

(a) Setup

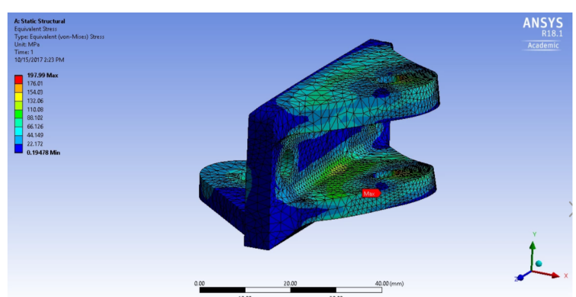

(b) Stress

Figure 41: Lower control arm clevis

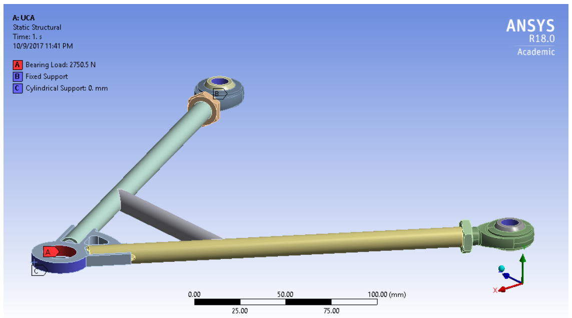

(a) Setup

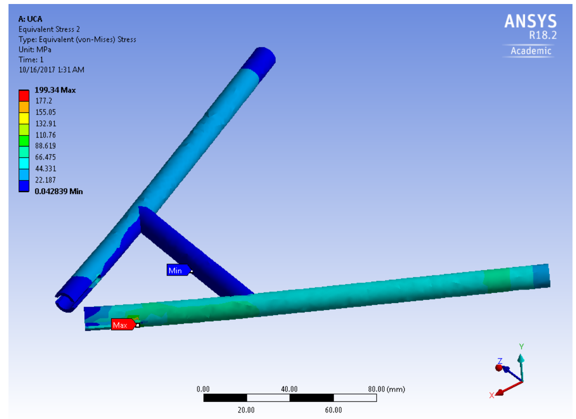

(b) Stress

Figure 42: Upper control arm

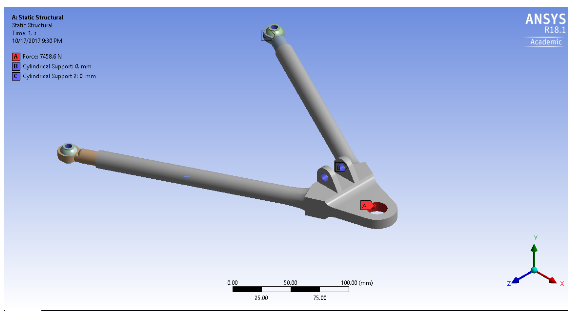

(a) Setup

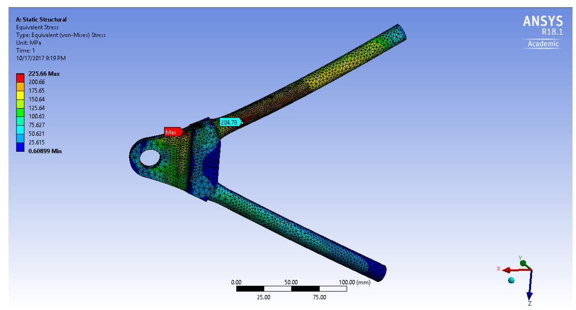

(b) Stress

Figure 43: Lower control arm

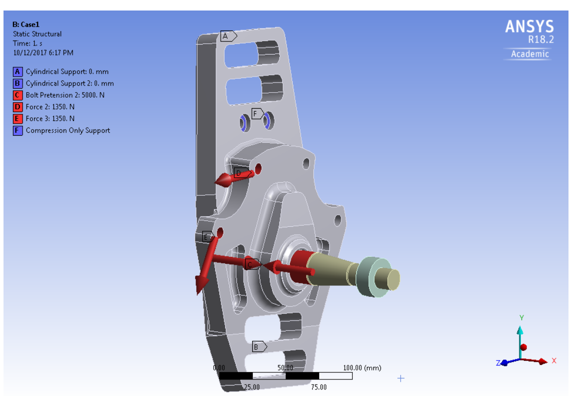

(a) Setup

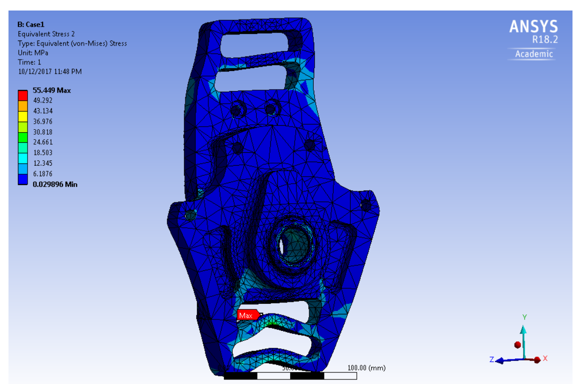

(b) Stress

Figure 44: Upright

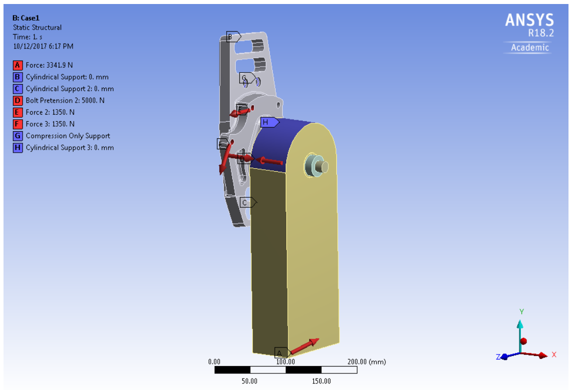

(a) Setup

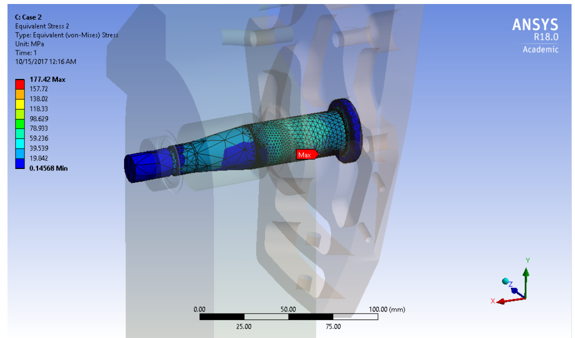

(b) Stress

Figure 45: Spindle

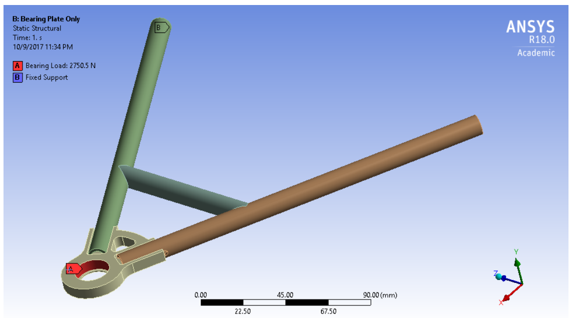

(a) Setup

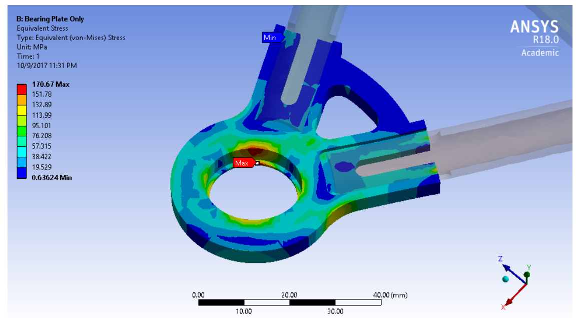

(b) Stress

Figure 46: Upper bearing plate

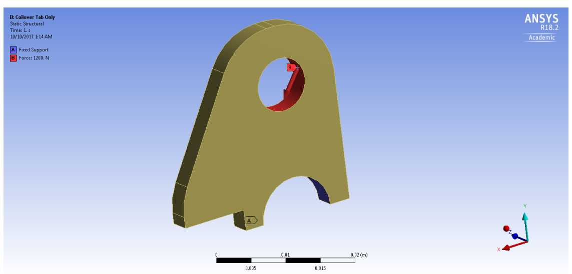

(a) Setup

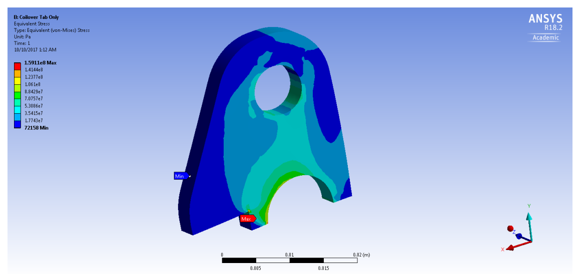

(b) Stress

Figure 47: Coilover control arm tab

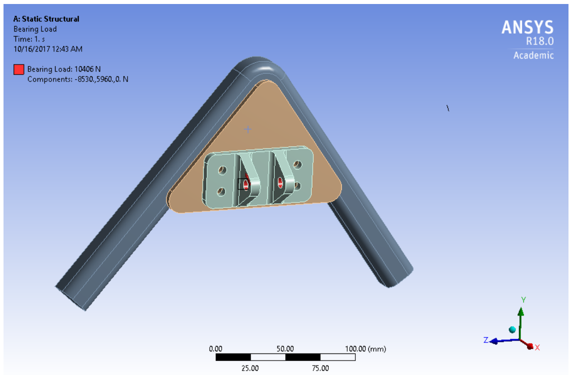

(a) Setup

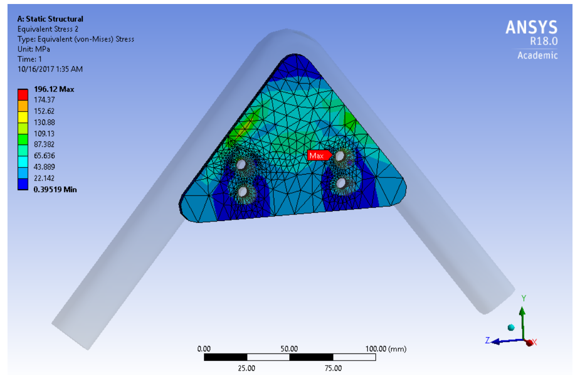

(b) Stress

Figure 48: Coilover mounting plate

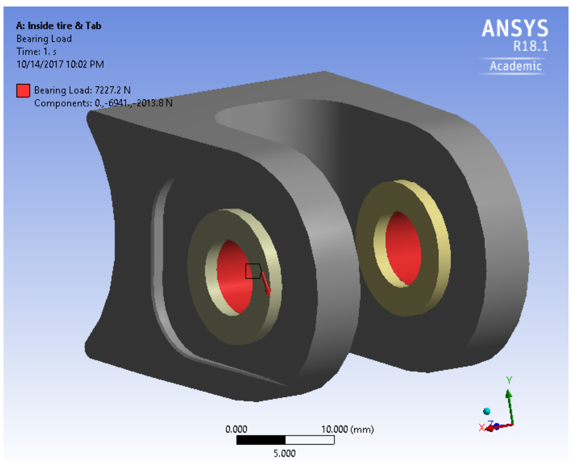

(a) Setup

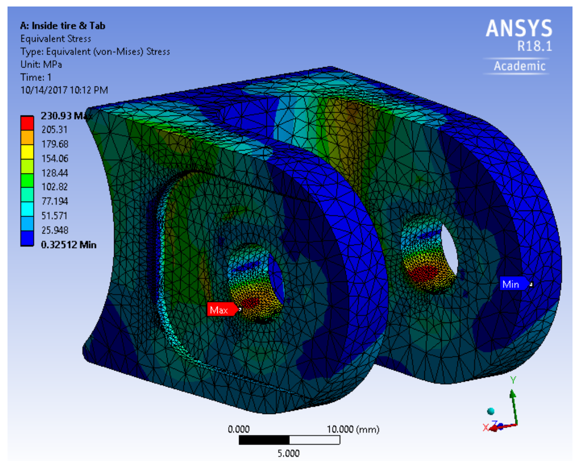

(b) Stress

Figure 49: Rear suspension clevis

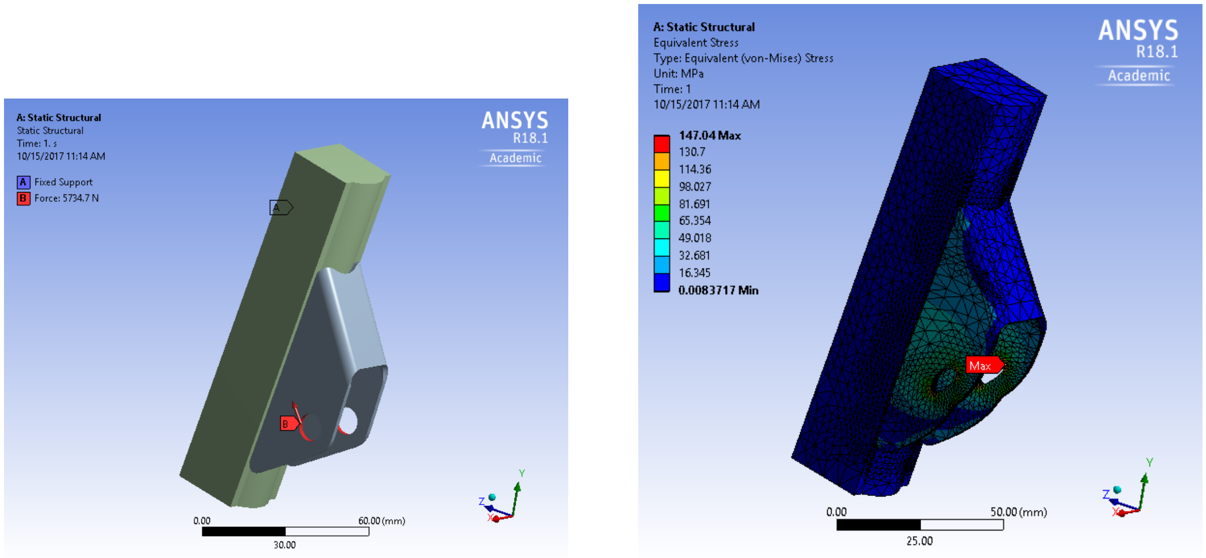

(a) Setup (b) Stress

Figure 50: Rear suspension coilover tab

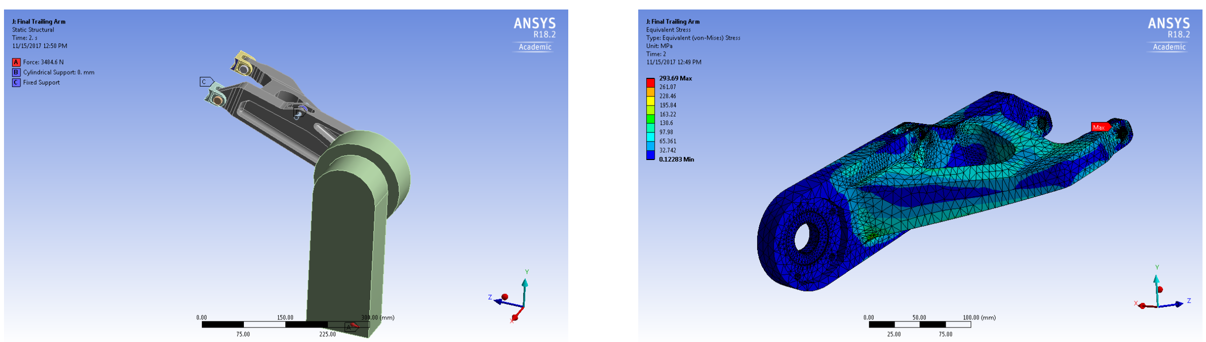

(a) Setup (b) Stress

Figure 51: Trailing arm

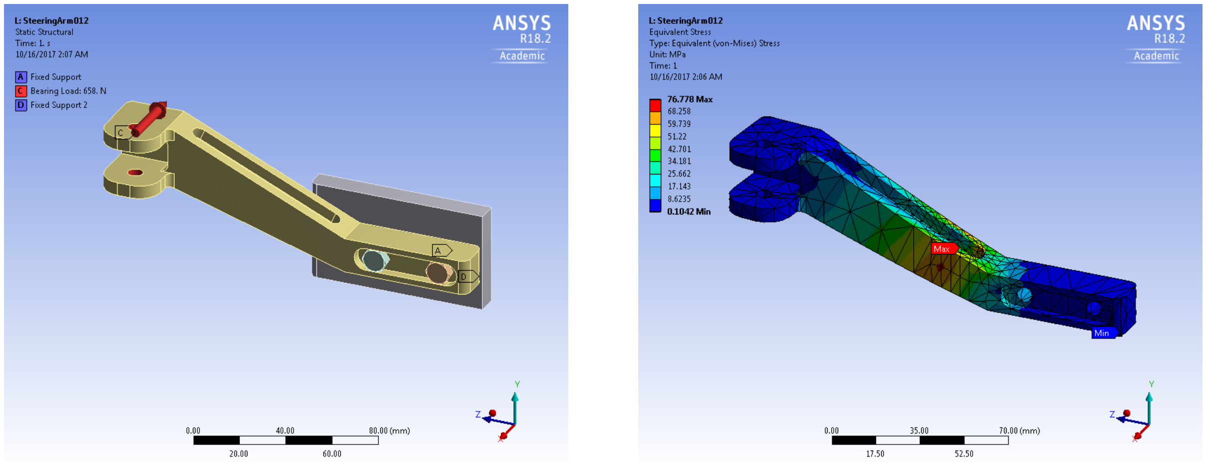

(a) Setup

(b) Stress

Figure 52: Steering arm

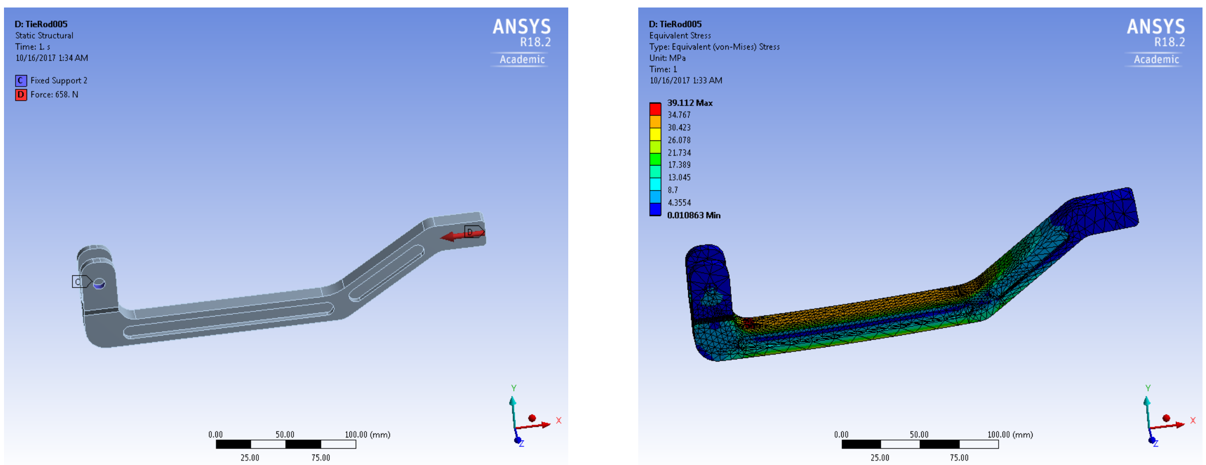

(a) Setup

(b) Stress

Figure 53: Tie rod